Aalborg Universitet

Flow Element Models

Heiselberg, Per; Nielsen, Peter V.

Publication date:
1996

Document Version
Publisher's PDF, also known as Version of record

[Link to publication from Aalborg University](#)

Supply Air Jet

Boundary Layer Flow

Convection Flow around Humans

Plume

Exhaust Flow

Gravity Currents

INDOOR ENVIRONMENTAL TECHNOLOGY
PAPER NO. 65

Chapter in "Ventilation of Large Spaces in Buildings - Part 3. Analysis and Prediction Techniques." To be published in 1997

P. HEISELBERG & P. V. NIELSEN
FLOW ELEMENT MODELS

INSTITUTTET FOR BYGNINGSTEKNIK
DEPT. OF BUILDING TECHNOLOGY AND STRUCTURAL ENGINEERING
AALBORG UNIVERSITET ● AAU ● AALBORG ● DANMARK

2.2 Flow Element Models

Air distribution in ventilated rooms is a flow process that can be divided into different elements such as supply air jets, exhaust flows, thermal plumes, boundary layer flows, infiltration and gravity currents. These flow elements are isolated volumes where the air movement is controlled by a restricted number of parameters, and the air movement is fairly independent of the general flow in the enclosure. In many practical situations, the most convenient method is to design the air distribution system using flow element theory. The flow element method is very useful in situations where the air flow pattern in a room is dominated by a single flow element or by flow elements that are not interacting with each other. In normal-size enclosures this is often true, so simple calculations using Flow Element models are all that is needed to design the air distribution system. In displacement ventilation, the supply of air from a low-level device and the thermal plume from heat sources above the floor are good examples of different flow elements that do not influence each other, and where the design of the air distribution system can be based on the models of these two flow elements. In large enclosures the airflow will often consist of several flow elements occurring at the same time. The flow elements will only dominate the air distribution in small parts of the enclosure and the flow path will often be influenced by other flow elements. Therefore, in large enclosures there will be large parts of the space where Flow Element models are not able to predict the air distribution. In such cases, Flow Element models will be useful only in the first stages of the design process, to keep design costs down, and possibly to estimate the airflow conditions in specific areas of the enclosure. More detailed analytical tools (field models) will be necessary to estimate the airflow and temperature conditions in the enclosure as a whole, but the results from Flow Element models will be very useful as initial input. The results can for example give an indication of where large gradients can be expected, so that a good distribution of local grid refinement can be made for CFD calculations.
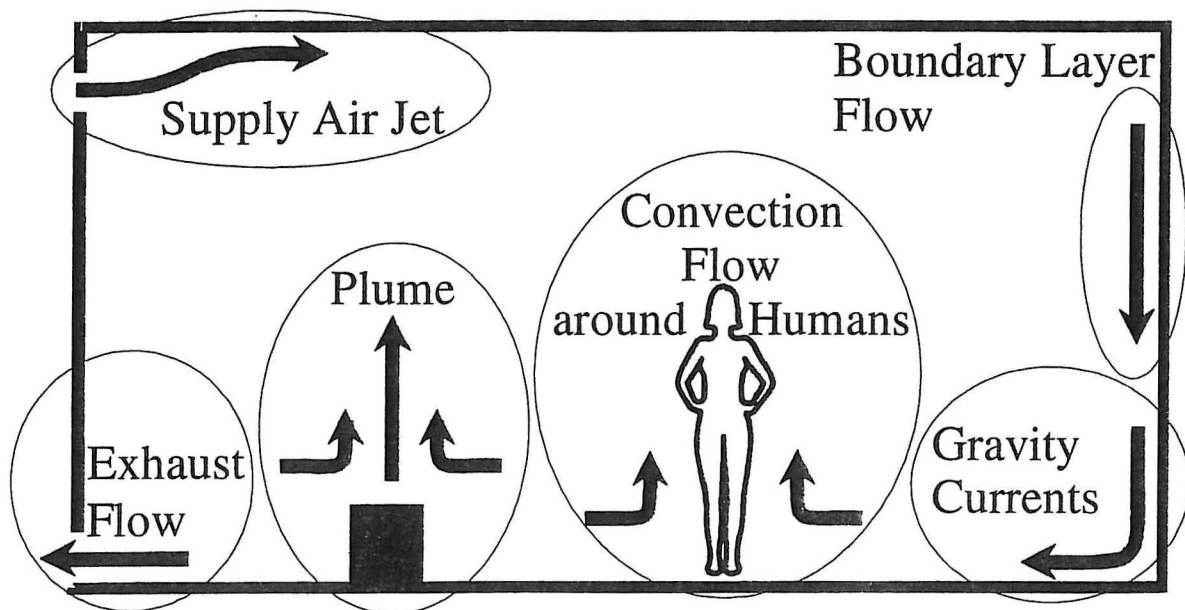

Figure 2.2.1   Examples of flow elements in ventilated spaces.

2.2.1 Isothermal and Thermal Jets

Air jets are often used to distribute the incoming air and to heat or cool the occupied zone in ventilated enclosures. In designing air distribution with jets, it is necessary to determine the jet trajectories, and the velocities and temperatures along the trajectories. This information is used to check that the jets will properly ventilate the occupied zone, with minimal discomfort. Depending on the type of air terminal device, the air jet can be characterised as a circular, plane or radial jet. In addition, the jet can be characterised as a free or wall jet depending on the location of the terminal device in relation to enclosing surfaces (Figure 2.2.2). A circular jet is generated from a circular, square or another concentrated outlet. A plane jet is generated from a slot or a row of closely spaced nozzles, while a radial jet is generated from an air terminal device that distributes the air radially. In practical situations, there can be different combinations of the above devices, which generate intermediate forms of these main jet types. Circular and radial air jets are most common, and generally the air is distributed by wall jets (along the ceiling) in small rooms, while large enclosures typically have free jets projected either vertically or horizontally into the enclosure. The work within Annex-26 has concentrated on vertical free jets.
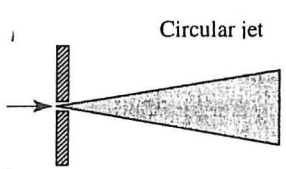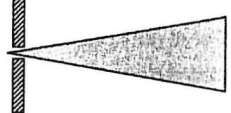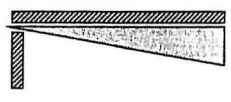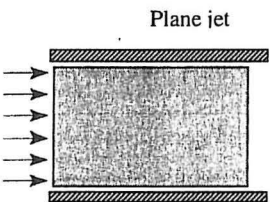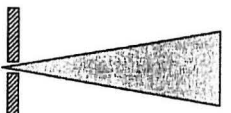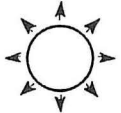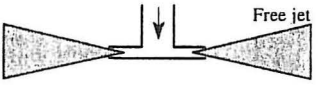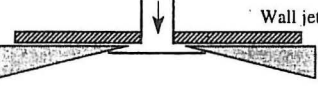
Top view	Side view	Velocity decay
Circular jet	Free jet	$u_x = u_o \dfrac{K_a}{\sqrt{2}} \dfrac{\sqrt{A_o}}{x}$ (m/s) (2.2.1)
	Wall jet	$u_x = u_o K_a \dfrac{\sqrt{A_o}}{x}$ (m/s) (2.2.2)
Plane jet	Free jet	$u_x = u_o \dfrac{K_p}{\sqrt{2}} \sqrt{\dfrac{h_o}{x}}$ (m/s) (2.2.3)
	Wall jet	$u_x = u_o K_p \sqrt{\dfrac{h_o}{x}}$ (m/s) (2.2.4)
Radial jet	Free jet	$u_x = u_o \dfrac{K_r}{\sqrt{2}} \dfrac{\sqrt{A_o}}{x}$ (m/s) (2.2.5)
	Wall jet	$u_x = u_o K_r \dfrac{\sqrt{A_o}}{x}$ (m/s) (2.2.6)

Figure 2.2.2   Different isothermal air jet types with corresponding velocity distribution.

Isothermal jets

A free jet is one that, in theory, flows into an infinitely large space, unhindered by obstructions. Likewise, a wall jet is one that flows along a surface bordering the space. These ideal jets, which are not influenced by downstream conditions, can be described by boundary layer approximations which give a self-similar flow with universal flow profiles; see Rajaratnam [*1976*]. These conditions are important because it enables us to describe the flow

in jets independently of the surrounding enclosure dimensions. It can be assumed that the initial flow momentum supplied at the air terminal device is preserved along the jet's trajectory. This leads to a simple relationship governing the velocity decay along the jet, shown in Figure 2.2.2. The constants K_a, K_p and K_r characterise the individual air terminal device. Typical values are K_a = 3-10, K_p = 2-4 and K_r = 1-2. The values can, as you can see, differ a great deal, and they are Reynolds-number dependent at low Reynolds numbers [*Nielsen and Möller, 1985, 1987, 1988*]. Therefore, it is advisable to use values measured at the actual air terminal device.

Horizontal thermal jets

Buoyancy will influence the flow in a jet if the air is supplied at a temperature different from the room temperature, as is the case when the air is used to heat or cool the space.

A horizontal projected nonisothermal free jet has a trajectory that curves downwards in the case of a cold jet (due to its higher density than surrounding air), and curves upwards in the case of a warm jet (due to buoyancy). The trajectory can be described by Equation (2.2.7) [*Koestel, 1955*]. The trajectory's geometrical co-ordinates, x and y, describe the curve traced out by the centre-line of the jet, i.e. the point of maximum velocity, and maximum or minimum temperature, for any given vertical cross section along the jet.
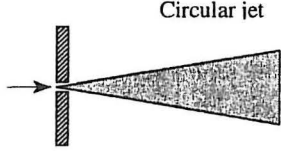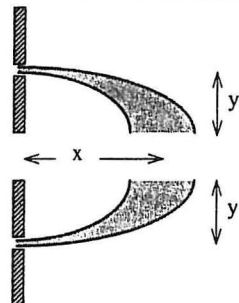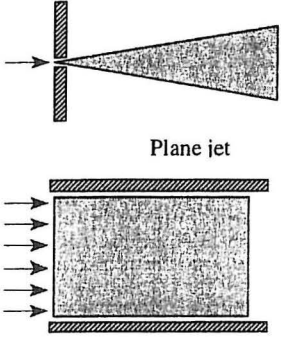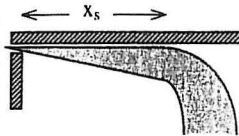
Top view	Side view	Trajectory/Penetration length
Circular jet	Free jet	$y = \dfrac{0.02}{K_a} \dfrac{\Delta T_o A_o}{u_o^2} \left(\dfrac{x}{\sqrt{A_o}} \right)^3$ (m) (2.2.7)
Circular jet Plane jet	Wall jet	$x_s = K_{sa} K_a \sqrt{\dfrac{u_o^2 \sqrt{A_o}}{\Delta T_o}}$ (m) (2.2.8) $x_s = K_{sp} K_p^2 \left(\dfrac{u_o^2 \sqrt{h}}{\Delta T_o} \right)^{2/3}$ (m) (2.2.9)

Figure 2.2.3   Trajectory and penetration length of horizontal thermal jets.

Also nonisothermal wall jets are influenced by gravity. However, the Coanda effect (see page 9) prevents the flow from detaching from the surface and following the free-jet trajectory described in Equation (2.2.7), until the jet reaches a certain distance, x_s, from the supply opening. When air-conditioning with ceiling wall-jets, a short penetration length, x_s, is undesirable, because a jet may have a high velocity and a low temperature when it flows down prematurely into the occupied zone, causing discomfort. The Coanda effect can thus be used to good effect in ventilation of large enclosures, by increasing throw length and preventing unwanted draughts in the occupied zone. A good example of this is the large jets used to

ventilate the terminal hall at Kansai International Airport, Japan [*Guthrie et al., 1992; Guthrie, 1996*].

Grimitlin [*1970*] and Schwenke [*1976*] have shown that the penetration length for a circular wall jet can be described by Equation (2.2.8) and for a plane wall jet by Equation (2.2.9); see Figure 2.2.3. The values of the constants K_{sa} and K_{sp} depend on parameters outside the jet, such as room dimensions, location of thermal load etc. [*Hestad, 1976*]. A value of $K_{sa} = K_{sp} = 1.5$ is valid for large rooms with an evenly distributed heat source over the whole floor area [*Nielsen and Möller, 1987, 1988*]. The values of K_a , K_p should be evaluated as described for isothermal jets.

The decay in centre-line velocity along a nonisothermal jet can be described by the same equation as used for the isothermal jet.

Thermal energy is preserved along a jet, in the same way as momentum, so it can be assumed that the temperature decay or increase along the jet's trajectory is proportional to the velocity decay (Equations (2.2.1 - 2.2.6) [*Nielsen and Möller, 1987*].

$$\frac{T_x - T_r}{T_x - T_o} \approx \frac{u_x}{u_o}$$
(2.2.10)

Vertical thermal jets

The velocity distribution in a vertical thermal jet depends on whether the momentum and gravity forces act in the same or opposite directions. In a jet where the forces are in opposition, the velocity decay is faster than in an isothermal jet, whilst it is slower in the reverse case. The velocity decay in a vertical circular jet is described by Equation (2.2.11) [*Koestel, 1954*], while Equation (2.2.12) gives an estimate for a vertical plane jet [*Regenscheit, 1970*]. In Equations (2.2.11) and (2.2.12) the plus sign is used when the momentum and gravity forces are in the same direction. The minus sign is used when they are in opposition.

A downward projected warm jet and an upward projected chilled jet have a limited penetration length, y_m, which corresponds to the distance where the velocity has fallen to zero. For a circular jet, the penetration length can be described by Equation (2.2.13) [*Helander et al., 1953*], and for a plane jet it can be roughly estimated by Equation (2.2.14) [*Regenscheit, 1959*].
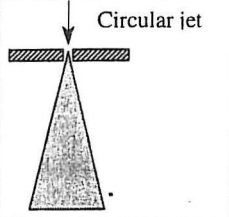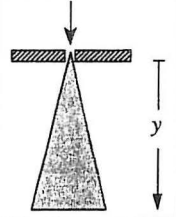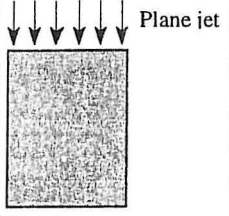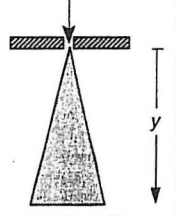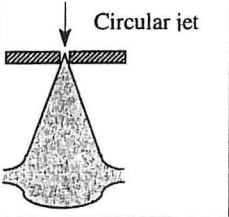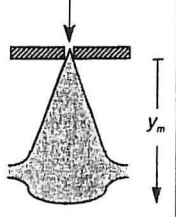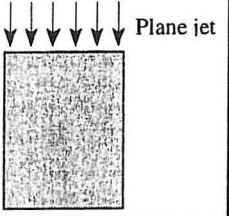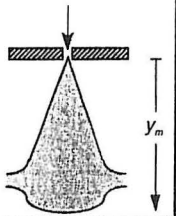
Front view	Side view	Velocity decay/Penetration length
Circular jet		Cold jet downwards Warm jet upwards use + sign $$v_y = v_o \frac{K_a}{\sqrt{2}} \frac{\sqrt{A_o}}{y}\left(1 \pm 0.09 \frac{|\Delta T_o|\sqrt{A_o}}{K_a v_o^2}\left(\frac{y}{\sqrt{A_o}}\right)^2\right)^{1/3} \quad \text{(m/s)} \quad (2.2.11)$$ Cold jet upwards Warm jet downwards use - sign
Plane jet		Cold jet downwards Warm jet upwards use + sign $$v_y = 2.5 v_o \sqrt{\frac{h_o}{y}} \pm 0.18 \sqrt{h_o|\Delta T_o|}\left(\sqrt{\frac{y}{h_o}} - 1\right) \quad \text{(m/s)} \quad (2.2.12)$$ Cold jet upwards Warm jet downwards use - sign
Circular jet		Cold jet upwards Warm jet downwards $\quad y_m = 3.33\sqrt{\dfrac{K_a v_o^2 \sqrt{A_o}}{|\Delta T_o|}}$ $\qquad$ (m) $\quad$ (2.2.13)
Plane jet		Cold jet upwards Warm jet downwards $\quad y_m = 19.2 h_o\left(\dfrac{v_o^2}{h_o|\Delta T_o|}\right)^{2/3}$ $\qquad$ (m) $\quad$ (2.2.14)

Figure 2.2.4   Velocity decay and penetration length for vertical thermal jets.

Vertical rectangular thermal jets

Very little results concerning 3D thermal free jets are available in the literature. Recently, an experimental study of 3D vertical free buoyant air jets was performed by Vialle and Blay [1996]. Decay laws were determined for 3D rectangular jets with positive buoyancy and penetration length were measured for jets with negative buoyancy. Results were obtained in the following parameter range: Jet aspect ratio: 4.4 (20 cm:4.5 cm); $0 < Ar < 0.3$; $3600 < Re < 12000$.

Jets with positive buoyancy

Several conclusions were drawn from this study. It was first found that the jet flow is not sensitive to Reynolds number but is very dependent on Archimedes number. Second, the centreline velocity and temperature decay slopes are depending on the Archimedes number defined as:

$$Ar = \frac{g\beta(T_0 - T_\infty)\sqrt{A}}{v_0^2} \qquad (2.2.15)$$

Second the jet flow can be divided into three zones depending on the dimensionless distance Y

5

$$Y = \frac{y}{\sqrt{A}} \tag{2.2.16}$$

where A is the inlet section area.

The three zones are defined as Zone 1 where the flow is establishing, (Y < 2), Zone 2 where the flow tends to behave as a plane jet, (2 < Y < 7), and Zone 3 where the flow tends to behave as an axisymmetrical jet, (Y > 7), see figure 2.2.5. Centreline velocity and temperature decay laws are given in table 2.2.1.
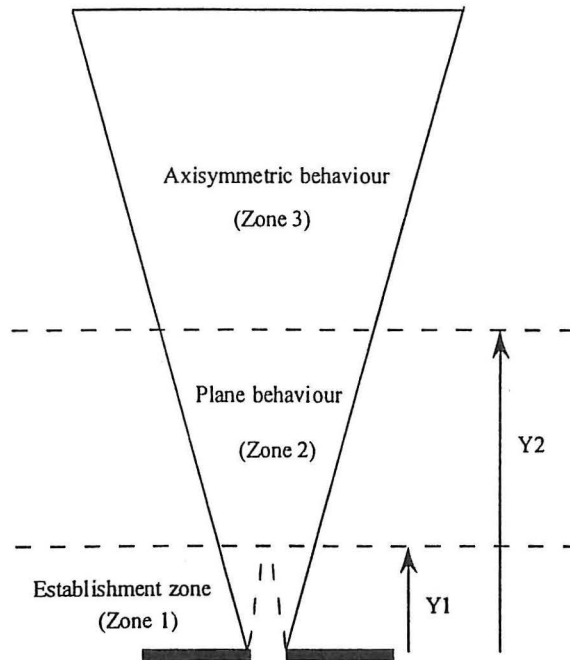
Figure 2.2.5   Side view of a rectangular vertical thermal jet with positive buoyancy.

Jets with negative buoyancy
For rectangular jets with negative buoyancy, penetration lengths were deduced from centreline velocity and temperature measurements. Results were obtained in the following parameter range: Jet aspect ratio : 4.4 (20 cm x 4.5 cm); 0.002 < Ar < 0.025; 6000 < Re < 12000. The penetration length is given by :

$$Y_m = 1.48 Ar^{-0.5} \tag{2.2.17}$$

Table 2.2.1   Velocity and temperature decay for vertical rectangular free thermal jets.

Zone		Velocity	Temperature
Zone 1 $0 < Y < Y_1$	$Y_1 = 2$	$v = v_0$	$T = T_0$
Zone 2 $Y_1 < Y < Y_2$	$Y_2 = 7$	$\dfrac{v}{v_0} = \left(\dfrac{Y_1}{Y}\right)^{b_2},$ $b_2 = 0.28\,\dfrac{0.22Ar + 0.07}{Ar + 0.07}$	$\dfrac{T - T_\infty}{T_0 - T_\infty} = \left(\dfrac{Y_1}{Y}\right)^{b_2},$ $b_2 = 0.28\,\dfrac{5.40Ar + 1.26}{Ar + 1.26}$
Zone 3 $Y > Y_2$	$Y_1 = 2$ $Y_2 = 7$	$\dfrac{v}{v_0} = \left(\dfrac{Y_1}{Y_2}\right)^{b_2}\left(\dfrac{Y_2}{Y}\right)^{b_3},$ $b_3 = 0.73\,\dfrac{0.203Ar + 0.028}{Ar + 0.028}$	$\dfrac{T - T_\infty}{T_0 - T_\infty} = \left(\dfrac{Y_1}{Y_2}\right)^{b_2}\left(\dfrac{Y_2}{Y}\right)^{b_3}$ $, b_3 = 0.73\,\dfrac{1.63Ar + 0.06}{Ar + 0.06}$

Behaviour of jets in confined spaces

The jets described by the Equations (2.2.1 - 2.2.17) are considered to be in an infinite isothermal medium. Depending on the room size, jets developing in real rooms are affected by wall and entrainment effects, which create substantial recirculation zones, as well as by thermal stratification.

In a deep room, an isothermal jet will have a restricted penetration length because entrainment generates a return flow in the room, so the jet gets dissolved after a certain distance. A jet can be considered to be developing freely as long as its cross section is less than 25% of the cross section of the room. The penetration length for a plane horizontal wall jet is given by Equation (2.2.21) [*Nielsen, 1976*]. The variation depends on the entrainment in the jet, where a high entrainment and a low K_p value give a short penetration length and a low entrainment and a high K_p value give a long penetration length [*Skåret, 1976*]. Equations (2.2.18 - 2.2.20) describe the penetration length of circular free, wall or corner jets, respectively [*Krause, 1972*].
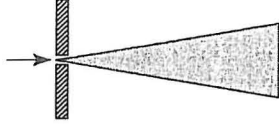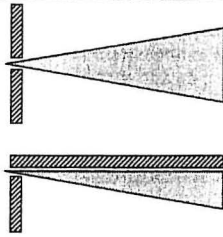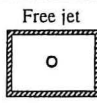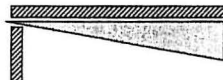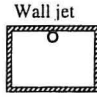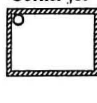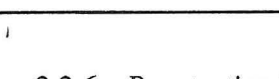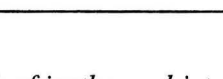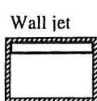
Top view	Side view	Front view	Penetration length
Circular jet		Free jet	$l_{re} = 3\sqrt{A}$ (m) (2.2.18)
		Wall jet	$l_{re} = 4.2\sqrt{A}$ (m) (2.2.19)
		Corner jet	$l_{re} = 6\sqrt{A}$ (m) (2.2.20)
Plane jet		Wall jet	$l_{re} = 3.0 - 5.3H$ (m) (2.2.21)

Figure 2.2.6   Penetration length of isothermal jets in deep rooms.

In a short room the jet will reach the end wall and be deflected towards the floor where it will turn 90° again and return along the floor. Experiments in conventional rooms ($L/H \approx 2-4$) with isothermal flow show that the maximum velocity in the reverse flow in the occupied zone, u_{rm}, is a simple function of a reference velocity, u_L, which is the velocity of an undisturbed wall jet at distance L from the actual diffuser. The velocity u_L contains information on supply velocity, distance from inlet and geometrical details that influence the initial flow, such as diffuser type and distance from ceiling. The ratio u_{rm}/u_L contains information on velocity decay in the deflected jet which is due to the end wall height and the geometry, as well as information on the velocity level in the recirculating flow which is due to the entrainment into the jet below the ceiling. For plane jet flow the ratio u_{rm}/u_L is rather independent of diffuser dimension and room height, and is equal to 0.7. A circular jet will be deflected downwards at the end wall as a semi-radial jet, so the ratio u_{rm}/u_L depends on the jet width compared with the width of the end wall. A small jet width ($< 0.5\ B$) results in a radial flow at the end wall and a ratio u_{rm}/u_L of 0.3, while a wide jet ($> 1.6\ B$) corresponds to plane jet flow and a ratio u_{rm}/u_L of 0.7 [*Hestad, 1976*]. New diffuser types with a specially designed semi-radial flow pattern may incorporate the side wall regions in the important part of the jet flow and this may result in values of u_{rm}/u_L above 0.7 in the occupied zone.

The behaviour of a nonisothermal free jet discharged into the open space is predicted rather well by the equations in Figure 2.2.3. However, Murakami *et al.* [*1991*] showed that it is not always possible for the equations to predict the trajectory of a jet discharged into an *enclosed* space. This is due to the fact that the air temperature around the jet is uniform in an open space while there is often a vertical temperature gradient in an enclosed space, as is the case in many large spaces. A temperature gradient means that the temperature in the lower region of the space differs from the temperature in the upper region. Thus the temperature difference between the jet and its surroundings is smaller in the lower region. Therefore, a chilled air jet in an enclosure will not fall as rapidly as it would in an open space with uniform temperature. Thermal jets developing in real rooms are also, depending on the room size, affected by wall and entrainment effects [*Grimitlin, 1970; Schwenke, 1975*].

When calculating the penetration length of nonisothermal wall jets in confined spaces, Equations (2.2.8) and (2.2.9) can be difficult to use in practice, because different air terminal devices produce different air flow patterns in the area where the jet leaves the ceiling region [*Nielsen and Möller, 1985, 1987, 1988*]. Jets from some diffusers may travel a further distance Δx_s along the ceiling (typically about 2-2.5 m) before they flow down into the occupied zone, while other wall jets leave the ceiling very abruptly.

Ceiling-mounted obstacles can influence the development of wall jets. Obstacles of large enough dimensions can deflect of the jet downwards prematurely, which can cause uncomfortable draughts and temperature differences in the occupied zone. A jet will be deflected down if the distance between the terminal and an obstacle of a given height is less than a critical distance, x_c. If the distance is equal to or greater than x_c, then the jet will reattach to the ceiling after passing the obstacle, and if the distance is more than 8 times x_c, then the wall jet will not be influenced at all by the obstacle. Room height also has an influence on the critical height, f_c, of an obstacle, because an initial deflection of a jet needs much space both in height and in the downstream direction to reattach itself to the ceiling. Figure 2.2.7 shows the critical height of an obstacle versus the distance from the diffuser for a plane wall jet [*Holmes and Sachariewicz, 1973; Nielsen, 1983*], and a for circular wall jet [*Nielsen et al., 1987*].
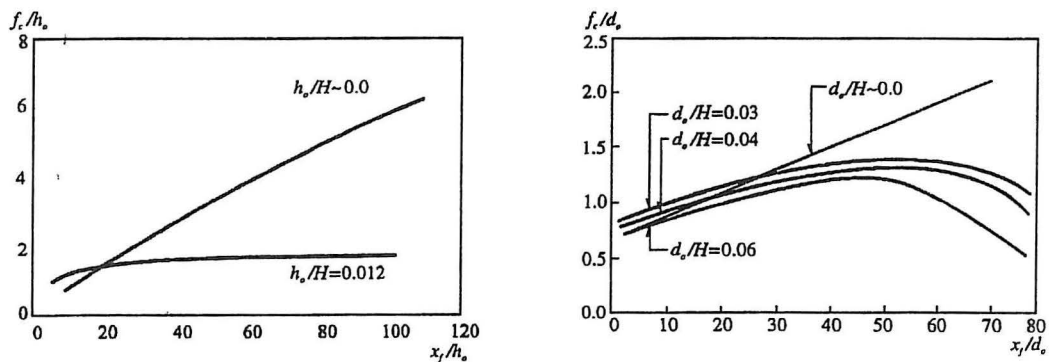
Figure 2.2.7   Critical height, f_c, of an obstacle versus distance, x_f, from the air supply terminal for (a) plane wall-jet flow and (b) circular wall-jet flow.

For nonisothermal flow, the critical height for ceiling-mounted obstacles also depends on the flow's Archimedes number in addition to the geometrical relations mentioned above. A chilled air jet will have a smaller the critical height while a warm air jet will have an larger critical height of the obstacle [*Söllner & Klingenberg, 1972; Nielsen, 1980*].

When a plane air jet or a circular air jet is injected parallel with and close to a surface, the turbulent mixing layer on both sides of the jet entrains air from the surroundings. A lower pressure on the side closest to the surface attracts the jet towards the surface, and so a wall jet is established at some distance from the supply terminal. The effect that generates this deflection is called the Coanda effect [*Jackman, 1970*]. There is no reliable information about the maximum distance where this effect can occur. It depends on the jet type and the air temperature, with a large maximum distance for plane and/or warm jets and a small maximum distance for circular and/or cool jets. The deflection reduces the jet's flow momentum; measurements made by McRee and Moses [*1967*] show that the final momentum can be reduced to 60-70 % of the inlet momentum, which means a reduced velocity level in the whole room.

A free jet that is injected at a certain distance and angle towards a surface will turn into a wall jet when it reaches the surface. This type of jet is called an impinging jet. The development of the wall jet will depend on the angle between the free jet and the surface. A

circular free jet will continue as a circular wall jet if the angle is small, and as a radial wall jet if the angle is large (~90°). This can be expressed by a change in the factor K_a as a function of the impingement angle, as in Figure 2.2.8 [Beltaos, 1976]. Equation (2.2.2) shows the development of the wall jet after impingement, and the appropriate K_a value can be taken from Figure 2.2.8.
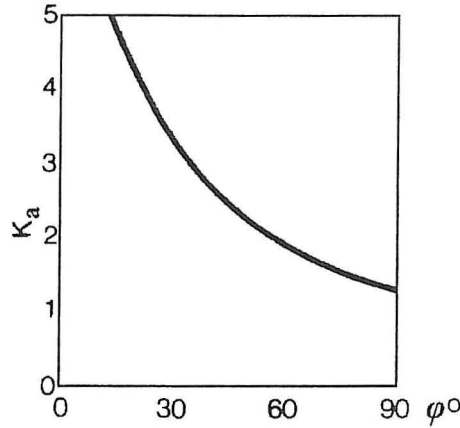
Figure 2.2.8 K_a values for an impinging circular jet as a function of the angle of impingement.

2.2.2 Thermal Plumes

Thermal plumes are created above everyday objects such as hot surfaces, equipment and persons, and they transport heat and air upwards from the lower region of a room to the upper region. In designing air distribution systems which use this effect, such as displacement ventilation, it is necessary to determine the amount of air which is transported, and in the case of temperature gradient in the space and/or distributed heat sources, how far the air reaches into the space. Buoyancy generates an upward jet-like flow with a maximum velocity just above the source, where the flow has its narrowest diameter. Air is entrained into the plume such that the width and the volume flow increase with height.

A concentrated heat source creates a circular flow while a line source creates a two-dimensional plane flow. The volume flow in a circular plume can be described by Equation (2.2.23) [Popiolek, 1996], which is based on the analysis of experimental data of several investigators. The equation is strictly valid for $y \gg d$ where d is the hydraulic diameter of the heat source. However, practice shows that the equation can be used down to a height of $y \approx 2d-3d$ [Kofoed and Nielsen, 1990]. The convective heat emission Φ_k can be estimated from the energy consumption of the heat source. For pipes and channels, the convective heat emission is about 70-90 % of the energy consumption. For smaller components it is about 40-60%, and for large machines and components it is about 30-50 %. The location of the virtual origin of the flow can in practice be very difficult to judge but, nevertheless, it is very important for an accurate estimate of the volume flow. It is often assumed that $y_0 \approx 2d$ for concentrated heat sources. In practical situations the position of the virtual origin of the flow can also be found on the basis of a measured (e.g. by smoke visualisation) maximum plume width at a certain distance from the heat source by Equation (2.2.22) [Popiolek, 1996]

$$y_0 = 2.6D_{max,1} - y_1 \quad \text{(m)} \tag{2.2.22}$$

The volume flow in a two-dimensional plume from a line heat source can be described by Equation (2.2.24) [*Skåret, 1986*]. In this case, the virtual origin y_o can be assumed to be 1-2 times the width of the heat source.

Influence of temperature gradient on plume development

Equations (2.2.23) and (2.2.24) are strictly only valid for homogeneous surroundings. If the surroundings have a vertical temperature gradient, the plume will have a lower velocity and volume flow compared with homogeneous surroundings, because the temperature gradient will diminish the buoyancy force. In a room with a pronounced temperature gradient, the buoyancy force will even become neutral at a certain height, y_t, but due to the momentum in the plume, it will continue a short distance until it has reached the maximum height, y_m. The flow will finally return to the height of neutral buoyancy, y_t, where it spreads out horizontally (Figure 2.2.9). Equations (2.2.25) and (2.2.26) can be used to find the values of y_m and y_t respectively [*Morton et al., 1956; Mundt, 1992*]. The flow rate, q_y, below height y_t is only moderately influenced by the temperature gradient.
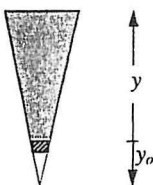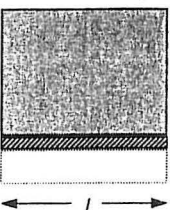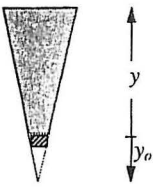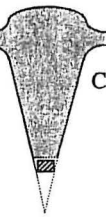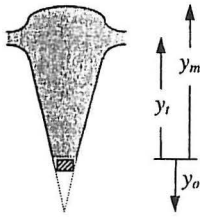
Front view	Side view	Volume flow/penetration height		
Circular plume		$q_y = 0.006\phi_k^{1/3}(y+y_o)^{5/3}$	(m³/s)	(2.2.23)
Plane plume		$q_y = 0.014\left(\dfrac{\phi_k^{1/3}}{l}\right)(y+y_o)l$	(m³/s)	(2.2.24)
Circular plume		$y_m = 0.98\phi_k^{1/4}\left(\dfrac{dT}{dy}\right)^{-3/8} - y_o$	(m)	(2.2.25)
		$y_t = 0.74\phi_k^{1/4}\left(\dfrac{dT}{dy}\right)^{-3/8} - y_o$	(m)	(2.2.26)

Figure 2.2.9   Volume flow and penetration height of thermal plumes.

Interaction between thermal plumes and influence of walls

If a heat source is close to a wall, then the resulting plume will be attached to the wall due to the Coanda effect. The rate of entrainment is then less than for a free plume. The wall can be considered as a symmetry plane, such that the flow will be similar to one half of the flow in a free plume of twice the convective heat emission. If the heat source is located close to a corner, similar assumptions may be applied, and so the plume can be considered as a quarter of a plume of four times the heat emission. The volume flow in a wall plume and a corner plume can be calculated from Equations (2.2.27) and (2.2.28) [*Nielsen, 1988; Kofoed and Nielsen, 1991*].

If a number of heat sources are located close to each other, then their thermal plumes may be absorbed into one large plume due to the Coanda effect. The flow from identical sources is given by Equation (2.2.29). The volume flow rate at a given height above two adjacent identical heat sources will only be 26% larger than the volume flow above one of the heat sources if it is separated from the other. In other words, the flow in a merged plume from a large number of heat sources is small compared with the flow in independent plumes with sufficient space for entrainment.
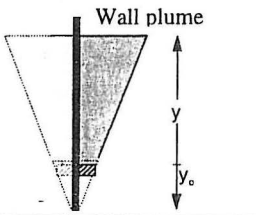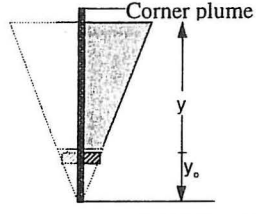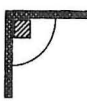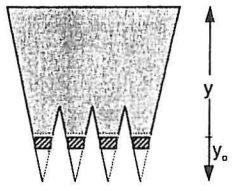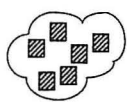
Side view	Top view	Volume flow
Wall plume		$q_{yw} = 0.0032\phi_k^{1/3}(y+y_o)^{5/3}$ (m^3/s) (2.2.27)
Corner plume		$q_{yc} = 0.002\phi_k^{1/3}(y+y_o)^{5/3}$ (m^3/s) (2.2.28)
Number of plumes		$q_{yN} = N^{1/3}q_y$ (m^3/s) (2.2.29)

Figure 2.2.10 *Volume flow in thermal plumes influenced by walls or plumes from other heat sources.*

Plume development in a confined space

The development of a plume in a confined space is affected by the geometry of the space and by the airflow in the space. In a tall slender space the cross-sectional area of the plume may grow to fill the whole cross-sectional area of the space, and then the plume will continue its vertical motion without entrainment. The height at which a confined flow is established can be calculated from Equation (2.2.30) [*Milke and Mowrer, 1995*].

$$y_c = 2.82\sqrt{A} \quad \text{(m)} \tag{2.2.30}$$

In spaces with a low ceiling height, the distance between the heat source and the ceiling might be too short for the plume to develop according to Equations (2.2.27 - 2.2.29). The minimum distance depends on the type and size of the heat source.

Depending on the conditions, the airflow in the space may act as a co-flow, boosting the velocity and volume flow rate in the plume, or may conversely reduce the velocity and the volume flow rate. A case with cold downdraught along the walls and a plume in the middle of the space is an example of a space with co-flow airflow conditions [*Kofoed and Nielsen, 1990*].

2.2.3 Free Convection Flows

Free convection flow arises at surfaces with a temperature different from the surroundings. Surfaces with temperatures different from the room air, are usually either poorly insulated or exposed to solar radiation. The work on free convection flows within Annex 26 has concentrated on cold surfaces, e.g. windows, where the important problem is to estimate the risk of draught in the occupied zone of the enclosure caused by cold downdraught along the glazing. This work focused on estimating maximum velocity and minimum temperature in the boundary layer, as well as the implications on the resulting thermal comfort in the occupied zone. This section discusses the results of the work on boundary layer flow, while the flow in the occupied zone is discussed in section 2.2.4 (Gravity Currents). The results may in most cases be equally applied to warm surfaces, with close accuracy.

The air adjacent to, for example a cold surface, will be cooled by conduction to the surface. This results in buoyant forces, causing the layer to flow downward. This layer of air adjacent to the surface, to which the vertical motion is confined, is called the natural convection boundary layer. The thickness of the boundary layer is zero at the top of the vertical surface, and increases in the downward direction due to entrainment of room air. If the surface is placed in calm surroundings, the boundary layer flow at the top of the surface will be laminar, and at a certain distance from the top it will become turbulent. The ratio between the buoyancy and viscous (friction) forces can be expressed by the Grashof number, defined as

$$\mathrm{Gr}_x = \frac{g\beta\Delta t_w x^3}{v^2} \qquad (2.2.31)$$

In experimental conditions typical of building enclosures [*Cheesewright, 1968; Cheesewright and Ierokiopitis, 1982*] the boundary layer flow is laminar for $\mathrm{Gr}_x < 1\times10^9$ and fully turbulent for $\mathrm{Gr}_x > 1.0\sim1.6\times10^{10}$. In large enclosures of considerable surface height, the flow is usually turbulent.

Free convection boundary layer flow on a vertical plane surface

The solution of the boundary layer equations for a vertical plane surface in both the laminar and the turbulent cases, after Eckert *et al.* [*1951, 1959*], gives equations for the maximum velocity, boundary layer thickness and volume flow, which are widely used in engineering applications. Laboratory measurements of the maximum velocity in boundary layer flows, Billington [*1966*], Howarth [*1972*], Shillinglaw [*1977*], and Topp and Heiselberg [*1996*], all show agreement with the theoretical dependence on surface height and temperature difference. However, they found lower velocity levels, i.e. values of the constant. The theoretical value of the constant [*Eckert and Jackson, 1951; Eckert and Drake, 1959*] was for laminar flow $k = 0.11$ and for turbulent flow $k = 0.10$, while the average values found in the measurements were $k = 0.09$ and $k = 0.07$, respectively. Table 2.2.2 shows equations for maximum velocity, average velocity, boundary layer thickness, volume flow rate, momentum flow and cooling/heating capacity of a boundary layer flow [*Andersen, 1996*]. In the table, the measured values are used for the maximum velocity and all the other theoretical relations are corrected according to that.

Table 2.2.2   Expressions for prediction of boundary layer flow at vertical plane walls.

	Laminar flow	Turbulent flow	
Maximum velocity (m/s)	$u_{max} = 0.09\sqrt{H\Delta T}$	$u_{max} = 0.07\sqrt{H\Delta T}$	(2.2.32)
Average velocity (m/s)	$u_{av} = 0.05\sqrt{H\Delta T}$	$u_{av} = 0.019\sqrt{H\Delta T}$	(2.2.33)
Boundary layer thickness (m)	$\delta = 0.048H^{1/4}\Delta T^{1/4}$	$\delta = 0.11H^{7/10}\Delta T^{-1/10}$	(2.2.34)
Volume flow rate (m³/s)	$q = 0.0024H^{3/4}\Delta T^{1/4}B$	$q = 0.0021H^{6/5}\Delta T^{2/5}B$	(2.2.35)
Momentum flow (N)	$I = 1.9\cdot10^{-4}H^{5/4}\Delta T^{3/4}B$	$I = 1.2\cdot10^{-4}H^{17/10}\Delta T^{9/10}B$	(2.2.36)
Cooling/heating capacity (W)	$\Phi = 1.2H^{3/4}\Delta T^{5/4}B$	$\Phi = 0.64H^{6/5}\Delta T^{1/4}B$	(2.2.37)

Free convection boundary layer flow on vertical surface with obstacles

Obstacles such as horizontal glazing frames, on a vertical surface, will influence the boundary layer flow depending on the characteristics of the flow and the size of the obstacles [*Heiselberg et al., 1995*]. If an obstacle is only small, then the boundary layer flow will reattach (or remain attached) to the surface after passing the obstacle. However, if the obstacle is sufficiently large, i.e. it exceeds a critical width, and if the flow conditions are transient or turbulent, then it will cause the boundary layer flow to separate permanently from the surface, and mix with the room air as a jet. A new boundary layer flow will then be established below the obstacle. In this way a high surface with regularly spaced obstacles will act as a collection of repeated individual flow units stacked on top of each other. The top units supply cold air to the room above the occupied zone, and the risk of draught in this zone will only be determined by the flow conditions at the lowest part of the facade [*Topp and Heiselberg, 1996*].

The critical width depends on the flow conditions at the wall. Under laminar flow conditions the critical width can be very large. Under transient and turbulent flow conditions, $Gr_x = 3\times10^9$ - 5×10^{10}, the critical width is about 0.25-0.30 m. If the size of the obstacle is below the critical width, the boundary layer flow will not separate from the wall. A recirculation zone will arise behind the obstacle and the boundary layer flow will at some distance reattach to the wall. However, the presence of the obstacle will reduce the maximum velocity in the boundary layer.

Figure 2.2.11 shows the expected development of the maximum velocity in the boundary layer flow according to Equation (2.2.32) at a plane surface of height of 3m and 6m, respectively. Further, velocities are given for measurements on a 6m high surface with obstacles 3m up which have widths of 0.1 m and 0.3 m.

The maximum velocity in the boundary layer flow measured just before the obstacle has the expected value. Below the obstacle, a new boundary layer flow is established, so for an obstacle of width 0.3 m, which exceeds the critical width, it will develop as would be expected for a 3m high plane surface. An additional increment of the obstacle width does not reduce the velocity level further. For an obstacle of width 0.1 m, which is below the critical width, the boundary layer flow reattaches to the surface, and the maximum velocity in the

boundary layer below the obstacle is higher than would be observed in a 3m high surface, but it is still below the level for a 6 m high plane surface.
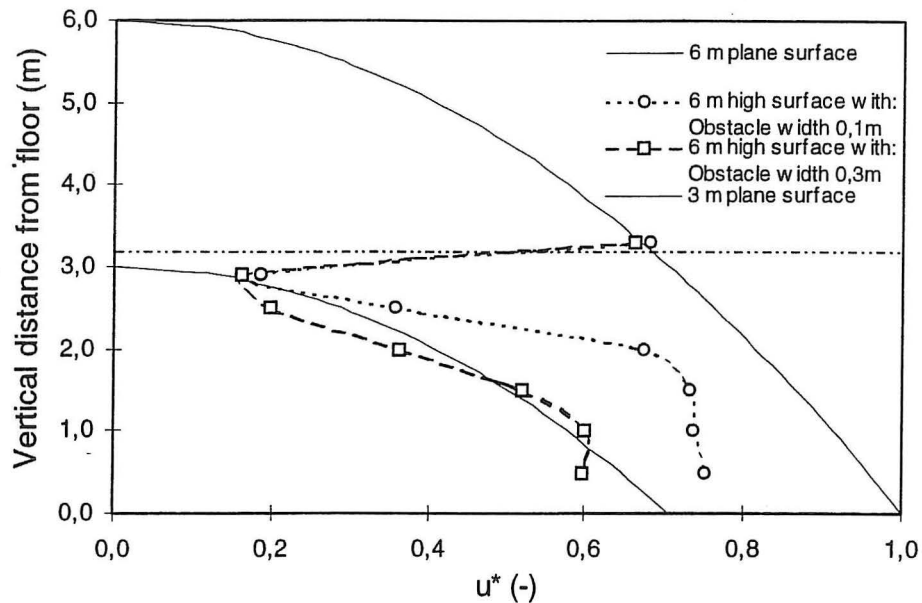

Figure 2.2.11 The measured maximum velocity in the boundary layer flow along a vertical surface with an obstacle of width above and below the critical width, respectively. Measurements are compared with the expected velocity along a plane surface with the heights of 3 m and 6 m. The temperature difference between the surface and the room was 9°C. [Topp and Heiselberg, 1996].

2.2.4 Gravity Currents

Gravity currents are primarily horizontal flows generated by small density differences, and governed by their negative buoyancy. The behaviour of a gravity current is therefore very much different from the behaviour of an air jet. For example the velocity increase above the supply velocity.

Examples of gravity currents generated within large enclosures are: airflow from low velocity devices in displacement ventilation, airflow from opening of doors to the outside or to another room where there is a temperature difference between the exterior and the interior air, and airflow along the floor from a vertical cold surface.

Wilkinson and Wood [*1970*] showed that a gravity current can be divided into three regions. In the first region the flow entrains fluid in a process similar to flow in a wall jet. This region is followed by a roller region after a certain distance, and the two regions together constitute what in hydraulics is known as a density jump. In the third region, downstream from the density jump, the entrainment fades. The flow in the entrainment region is called supercritical flow, and in the area with diminishing entrainment it is called subcritical flow.

It has not been possible to identify all these elements in the flow from low velocity devices and air flows induced by free convection flows at vertical walls, but the decreasing entrainment coefficient as a function of the distance or the local Archimedes number has been identified for gravity currents in rooms [*Nielsen, 1994a; Sandberg and Mattsson, 1993; Heiselberg, 1994a*].

Air supply from low velocity devices
In displacement ventilation, air is supplied directly into the occupied zone. The supply openings may either be mounted in the floor producing vertical free jets directed upwards, or they are located along the walls as low velocity air terminal devices. Floor-mounted diffusers must generate very high entrainment to keep the velocity level low close to the inlet. This is usually achieved by supplying a swirl to the flow [*Nielsen et al., 1988*]. Another possibility is to adopt the whole floor as the supply area, as shown by Akimoto *et al.* [*1995*]. At large Archimedes numbers the cold air from a wall-mounted low velocity air terminal device accelerates towards the floor due to gravity, and it behaves like a gravity current as it progresses along the floor. This airflow influences the thermal comfort of the occupants, so it is vital to estimate the maximum velocity of the flow along the floor. The velocity level depends on the flow rate to the room, the temperature difference and the type of air terminal device, where especially the height of the device is an important parameter.

The flow from a single air terminal device will be radial partly due to the gravity effect and partly due to the construction of the device, and it will have an almost constant thickness across most of the floor. The maximum velocity, u_x, in the symmetry plane of the flow at distance x is given by Equation (2.2.38) [*Nielsen, 1994a*].

$$u_x = q_o K \frac{1}{x} \quad \text{(m/s)} \tag{2.2.38}$$

The parameter K (m^{-1}) is given by the diffuser design and the ratio

$$\frac{(T_{oc} - T_o)}{q_o^2} \quad (°C \cdot s^2/m^6) \tag{2.2.39}$$

The temperature difference (T_{oc}-T_o) is between the temperature at the height of 1.1 m and the supply temperature. The ratio in Equation (2.2.39) can be regarded as a part of an Archimedes number.

Figure 2.2.12 shows the parameter K versus the ratio given by Equation (2.2.39). The K-value for an air terminal unit with an axial air supply is located in the upper part of the graph. The flow is axial at small temperature differences. The gravity effects turn the flow into a radial pattern at high Archimedes numbers. The upper part of the graph is typical of air terminal devices with a radial/axial velocity distribution, and the lower part of the graph is typical of diffusers with a 'flat' velocity distribution at the diffuser surface [*Nielsen, 1992, 1994a*]. Figure 2.2.12 is based on diffusers with a height up to 1.0 m and an area up to 0.5 m^2. Equation (2.2.38) is valid for distances larger than 1.0-1.5 m from the air terminal device.
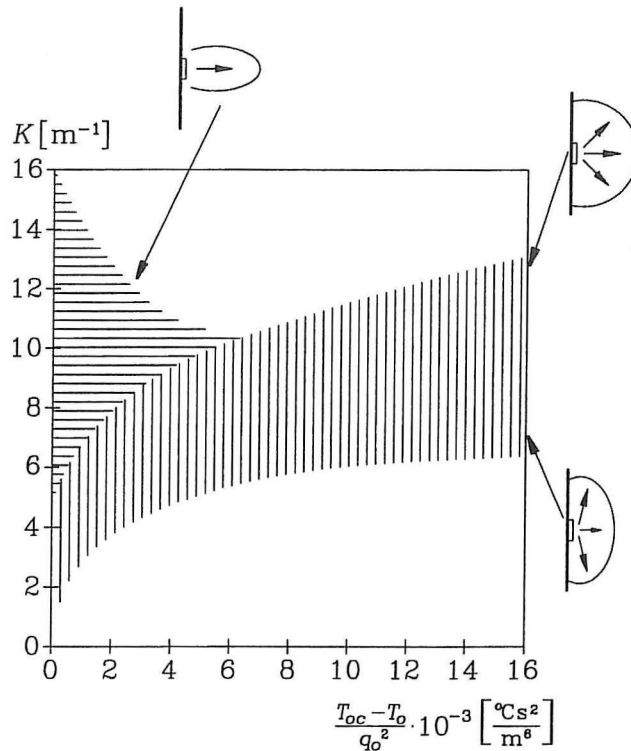
Figure 2.2.12 K-values for low velocity air terminal devices as a function of air flow and temperature difference [Nielsen, 1992, 1994a].

Airflow induced by convective flow along vertical walls

Free convection flows at surfaces with a temperature lower than the surroundings will produce airflow along the floor. The main concern for such flow is estimating of the risk of draught in the occupied zone and consequently the estimation of the parameters' maximum velocity and minimum temperatures in the flow.

Measurements by Heiselberg [*1994a*] have shown that the airflow along the floor can be divided into three different zones. The first zone is near the foot of the vertical wall, where the flow turns from a vertical boundary layer flow to horizontal airflow. In the second zone, the flow entrains room air and develops like a wall jet. Here the maximum velocity decreases and the height of the flow increases proportionally with the distance from the virtual origin of the flow. Due to buoyancy, the flow gradually changes and the entrainment rate of room air decreases. In the third zone, both the height of the flow region and the maximum velocity are constant and the entrainment rate of room air is very small.

In a two-dimensional airflow situation the Equations (2.2.40 - 2.2.43) give the maximum velocity and the minimum air temperature in the near floor region of the airflow as a function of the distance to the cold vertical wall, the height of the wall, and the temperature difference between the cold wall and the occupied zone.

$$u_{\max}(x) = 0.055\sqrt{H \cdot \Delta T} \qquad \text{(m/s)}, \quad x < 0.4 \text{ m} \qquad (2.2.40)$$

$$u_{\max}(x) = 0.095\frac{\sqrt{H \cdot \Delta T}}{x + 1.32} \qquad \text{(m/s)}, \quad 0.4 \text{ m} \le x \le 2.0 \text{ m} \qquad (2.2.41)$$

$$u_{\max}(x) = 0.028\sqrt{H \cdot \Delta T} \qquad \text{(m/s)}, \quad x > 2.0 \text{ m} \qquad (2.2.42)$$

17

$$T_{\min}(x) = T_r - (0.30 - 0.034x)\Delta T \quad (K) \qquad\qquad (2.2.43)$$

The expressions are valid for conditions at the cold vertical surface corresponding to Grashof numbers between 1.12×10^{10} - 3.85×10^{10}, which means that the boundary layer flow at the surface is in the fully turbulent region. The expressions should be used with caution considering that the room geometry influences the development of the flow along the floor. The experiments were performed in a room which was 7 m deep. In a three-dimensional situation, the velocity at the symmetry plane of the airflow along the floor is approximately the same as in the ideal two-dimensional situation. These expressions were compared with measurements of draught in a real atrium, as part of Annex-26; see Section 4.6.3.
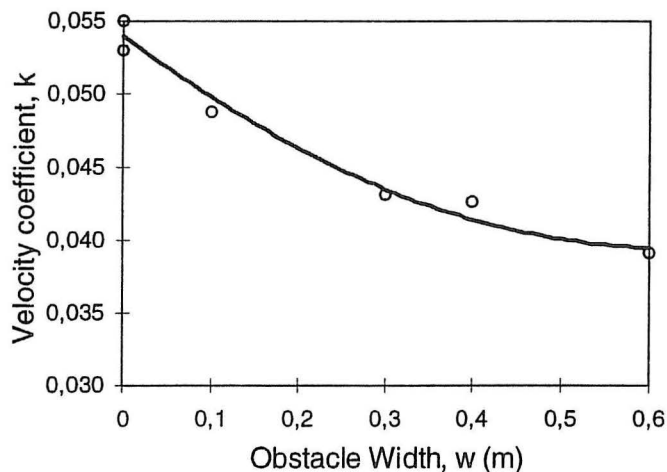

Figure 2.2.13 Maximum velocity in the occupied zone, expressed by the coefficient k, as a function of obstacle width for a 6 m high vertical surface with a horizontal obstacle positioned at 3 m height. The temperature difference between the surface and the room was 9°C. [Topp and Heiselberg, 1996].

The presence of an obstacle on a wall will reduce the maximum velocity in the boundary layer flow and the velocity level in the occupied zone. The larger the obstacle is, the larger the reduction in the velocity level will be. Figure 2.2.13 shows the reduction of the maximum velocity in the occupied zone as a function of the obstacle width expressed by the reduction in the constant, k, in Equation (2.2.40). The constant is reduced from $k = 0.055$ for a plane surface to $k = 0.040$ for a surface with an obstacle with the width of 0.6 m. The velocity level in the occupied zone found by Equation (2.2.40) and a constant of 0.040 corresponds to the velocity level in the occupied zone caused by a 3m high surface. Therefore, an increase in the obstacle width will not give a further decrease in the velocity level in the occupied zone.

The velocity will only be reduced close to the wall ($x < 1.0$-1.5 m) where the level and consequently the risk of draught is highest, while there is almost no reduction in the velocity level further from the wall, ($x > 2.0$ m).

2.2.5 Exhaust Flows

The air movement in the vicinity of a return opening is called a potential flow. Air moves in a virtually straight line towards the opening (sink) from all directions. This contrasts with the situation near a supply opening, where the jet flow is highly directional due to the conservation of momentum. Consequently, the velocity at a given distance from an extract opening is much lower than the maximum velocity of a supply jet of the same volume flow.

Naturally, momentum flow is also preserved at an extract opening. A wall jet flow which passes near an extract grille will only be slightly deflected because the return grille generates small velocities compared with the velocity in the wall jet. The air that is removed by the return grille will mainly be mixed room air because the jet has a high entrainment and, therefore, contains a high fraction of recirculated room air. Short-circuiting of air is therefore avoided even in cases with a short distance between the supply and extract, for isothermal flow.

Although the extract opening has only a small influence on the velocity level in the room, it may have large influence on the ventilation effectiveness. In order to prevent short-circuiting, the extract must have a high location if the room is ventilated by chilled jets and a low location if the room is heated by a warm air system. Extract openings can also be used to control the pressure distribution in a room or in a building. It is possible to keep contaminated air in a part of a building by extracting enough air in that region to control the pressure distribution. For example, this principle can enclose a catering section in a large room.

An extract opening in a plane surface will, in case of isothermal surroundings, generate a velocity, u_x, at a distance x from the opening as given by Equation (2.2.44). The equation shows that the velocity will be very small at a short distance from the opening.
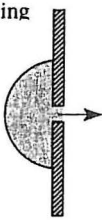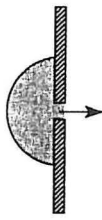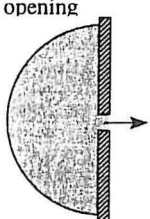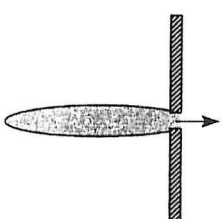
Top view	Side view	Velocity distribution
Exhaust opening		Isothermal surroundings $u_x = \dfrac{q_E}{A_E + 2\pi x^2}$ (m/s) (2.2.44)
Exhaust opening		Surroundings with thermal stratification

Figure 2.2.14 Velocity distribution in front of an exhaust opening in case of isothermal surroundings and surroundings with temperature stratification.

When a temperature gradient is present, the flow in front of an exhaust opening will change, as illustrated in Figure 2.2.14 [*Skistad, 1994*]. Horizontal air movement will be more pronounced than vertical air movement, because the flow must act against the buoyancy forces in the latter case. This effect can be used as a flow element in industrial areas. Skistad [*1993*] showed how it is possible, by the correct location of the exhaust openings, to divide a large ship building hall with displacement ventilation into a contaminated part and a part with clean air. Combined heat and contaminant sources often generate a layer of contaminated air in a tall room with a vertical temperature gradient, and it is therefore very efficient to locate the exhaust opening close to this height.

2.2.6 Interaction between Flow Elements

In large enclosures, which often have a complicated geometry, different flow elements occur at the same time, and they may influence each other's flow path. The resulting airflow pattern in the enclosure depends on the individual strength of each element and on the way they act together. It is therefore necessary, during the design of the air distribution system, not only to determine the jet trajectories but also to take into account all sources of air movement, in order to assess whether the interaction between the flow elements changes the flow paths of individual elements, and to estimate if this affects the overall airflow pattern and efficiency of the ventilation system.

In a series of scale model experiments, it was investigated how different flow elements such as horizontal air jets, thermal plumes and free convection flows interact with each other in a large enclosure [*Heiselberg, 1994b*]. The main emphasis was put on the pathway of chilled horizontal free air jets, and whether the convective flows from both distributed and concentrated heat sources affected the pathway of the jet and the air flow pattern in the enclosure as a function of the location of the heat source and as a function of the heat supplied by the source.

The experiments showed that the penetration depth and the paths of cold jets in enclosures were not influenced by the presence of distributed heat sources, e.g. a heated floor or a heated part of the floor, and were only slightly influenced by the presence of concentrated heat sources. In the latter case the air jet entrained the warm air from the plume above the heat source giving higher temperatures in the jet and therefore it did not fall as rapidly as expected.

As regards the overall flow in the enclosure, the experiments showed that at low Archimedes numbers for the jet, the airflow pattern in the enclosure was determined by the supply air jet. At higher Archimedes numbers, where the strength of the jet was smaller, the pathway of the jet was still independent of the type and location of the source. However, the experiments showed that the airflow pattern in the enclosure was increasingly determined by the convective flows from the heat sources. This means that the thermal comfort and the risk of draught in the occupied zone, because of low temperatures and high velocities in the supply air jet, can be estimated from traditional jet theory, while the air quality and the ventilation effectiveness in the occupied zone depend also on the type, location and strength of the heat sources.

2.2.7 Summary

Flow elements are isolated volumes of the enclosure where the air movement is controlled by a restricted number of parameters, and the air movement is fairly independent of the general flow in the enclosure. This subchapter contains a selection of the most important models for flow elements. The development of these semi-empirical models is based on comprehensive measurement work and experience, but they are often constrained to simplified geometrical and physical conditions. Therefore, Flow Element models give very good predictions in cases that closely match the experimental conditions, while it can be difficult to apply them and get accurate predictions in cases that differ. The greatest assets of these models are that they are easy and fast to use, they require only a few input parameters, and they do not need any investment to use. To apply the models on a particular case, it is necessary first to define the geometrical and physical conditions, to find the appropriate model, to estimate the input parameters and to calculate the results using a pocket calculator or a spreadsheet program. However, at the same time this is the models' greatest disadvantage. Many of the models are only applicable under certain conditions, and together with the limited requirements to the input parameters, the results will not give very detailed information on the airflow conditions but only on the level of a few key parameters of the flow.

Conventionally sized enclosures typically have simple geometry and physical conditions, and the airflow is usually dominated by a single flow element or by flow elements that do not interact with each other. Therefore, an analysis of the airflow by Flow Element models is sufficient in the design of the air distribution system.

Large enclosures on the other hand, often have very complicated geometry and physical conditions, and the airflow is often driven by several flow elements. Flow elements dominate the airflow only locally in relatively small regions of the enclosure and their flow paths are often influenced by other flow elements. In such cases, Flow Element models are useful only in the first stages of the design process, to keep design costs down, and possibly to estimate the airflow conditions in specific areas of the enclosure. More detailed analytical tools (field models) are necessary to estimate the airflow and temperature conditions in the enclosure as a whole. However, Flow Element models are still a very useful guide for comparison and as input when using more advanced models.

References

Akimoto, T.; Nobe, T.; Takebayashi, Y. [1995]: Experimental Study on the Floor-Supply Displacement Ventilation System. *ASHRAE Transactions, Vol 101, Pt. 2.*

Andersen, K.T. [1996]: SBI Bulletin 112: Cold Down-Draught from Cold Surfaces (in Danish). *Danish Building Research Institute.*

Beltaos, S. [1976]: Oblique impingement of circular turbulent jets. *Journal of Hydraulic Research, Vol 14, no. 1.*

Billington, N.S. [1966]: Air Movement over Hot or Cold Surfaces. *Laboratory Report no. 29, HVRA.*

Blay, D.; Vialle, P. [1996]: Experimental Study of Free Buoyant 3D Jets. *Internal Report, Laboratoire d'Etudes Thermiques, ENSMA, University of Poitiers, France.*

Cheesewright, R. [1968]: Turbulent Natural Convection from a Vertical Plane Surface. *Journal of Heat Transfer, Vol. 90, pp 1-8.*

Cheesewright, R.; Ierokiopitis, E. [1982]: Velocity Measurements in a Turbulent Natural Convection Boundary Layer. *Int. Heat Transfer Conference, 7, Munich, Vol. 2.*

Eckert, E.R.G. and Drake, R.M. [1959]: Heat and Mass Transfer. *McGraw-Hill.*

Eckert, E.R.G.; Jackson, T.W. [1951]: Analysis of Turbulent Free-convection Boundary Layer on Flat Plate. *NACA Report 1015.*

Grimitlin, M. [1970]: Zuluftverteilung in Räumen, Luft- und Kältetechnik. *No. 5.*

Heiselberg, P. [1994a]: Stratified Flow in Rooms with a Cold Vertical Wall. *ASHRAE Transactions, Vol. 100, part 1, pp 1155-1162.*

Heiselberg, P. [1994b]: Interaction between Flow Elements in Large Enclosures. *Proc. of the Fourth International Conference on Air Distribution in Rooms, ROOMVENT '94, Krakow, Vol. 1, pp 363-376.*

Heiselberg, P.; Overby, H.; Bjoern, E. [1995]: Energy-Efficient Measures to avoid Downdraft from Large Glazed Facades. *ASHRAE Transactions, Vol. 101, pp .*

Helander, L.; Yen, S.M.; Crank, R.E. [1953]: Maximum Downward Travel of Heated Jets from Standard Long Radius ASME Nozzles. *ASHVE Transactions, No. 1475.*

Hestad, T. [1976]: Dimensioning of Supply Openings, Cold Downdraught (in Norwegian). *Norsk VVS, No. 6.*

Holmes, M.J. and Sachariewicz, E. [1973]: The Effect of Ceiling Beams and Light Fittings on Ventilating Jets. *Laboratory Report No. 79, HVRA.*

Howarth, A.T. et al. [1972]: Air Movement in an Enclosure with a Single Heated Wall. *B.S.E., Vol. 40, pp 149-156.*

Jackman, P.J. [1970]: Air Movement in Rooms with Sidewall Mounted Grilles - A Design Procedure. *Laboratory Report No. 65, HVRA.*

Koestel, A. [1955]: Paths of Horizontally Projected Heated and Chilled Air Jets. *ASHRAE Transactions.*

Koestel., A. [1954]: Computing Temperatures and Velocities in Vertical Jets of Hot or Cold Air. *Heating, Piping & Air Conditioning, June.*

Kofoed, P.; Nielsen, P.V. [1990]: Thermal Plumes in Ventilated Rooms. *Proc. of the International Conference on Engineering Aero- and Thermodynamics of Ventilated Room, ROOMVENT '90, Oslo.*

Kofoed, P.; Nielsen, P.V. [1991]: Auftriebsströmungen verschiedener Wärmequellen - Einfluss der umgebenden Wände auf den geförderten Volumenstrom. *DKV-Tagungsbericht, Deutscher Kälte- und Klimatechnischer Verein e.V., Stuttgart.*

Krause, D. [1972]: Freistrahlen bei der Sonderbewetterung. *Neue Bergbautechnik, 2 Jg, Heft 1.*

Li, Z.H.; Zhang, J.S.; Zhivov, A.M.; Christianson, L.L. [1993]: Characteristics of Diffuser Air Jets and Airflow in the Occupied Regions of Mechanically Ventilated Rooms - A Literature Review. *ASHRAE Transactions, Vol. 99, part 1, pp 1119-1127.*

McRee, D.I. and Moses, H.L. [1967]: The Effect of Aspect Ratio and Offset on Nozzle Flow and Jet Reattachment. *Advances in Fluidics, The 1967 Fluidics Symposium, ASME.*

Milke, J.A. and Mowrer, F.W. [1995]: Computer Aided Design for Smoke Management. *ASHRAE Journal, August 1995.*

Morton, B.R.; Taylor, G.; Turner, J.S. [1956]: Turbulent Gravitational Convection from Maintained and Instantaneous Sources. *Proc. Royal Soc., Vol. 234A, p. 1.*

Mundt, E. [1992]: *Convection Flows in Rooms with Temperature Gradients - Theory and Measurements. Proc. of the Third International Conference on Air Distribution in Rooms. ROOMVENT '92, Aalborg.*

Murakami, S.; Kato, S.; Nakagawa, H. [1991]: Numerical Prediction of Horizontal Nonisothermal 3-d Jet in Room based on the k-ε model. *ASHRAE Transaction, Vol. 97, Part 1, pp 96-105.*

Nielsen, P.V.; Evensen, L.; Grabau, P.; Thulesen-Dahl, J.H. [1987]: Air Distribution in Rooms with Ceiling-Mounted Obstacles and Three-Dimensional Isothermal Flow. *ROOMVENT'87, International Conference on Air Distribution in Ventilated Spaces, Stockholm, 1987.*

Nielsen, P.V. [1976]: Flow in Air Conditioned Rooms - Model Experiments and Numerical Solution of the Flow Equations. *English translation of Ph.D.-Thesis, Technical University of Denmark, Copenhagen.*

Nielsen, P.V. [1980]: The Influence of Ceiling-Mounted Obstacles on the Air Flow Pattern in Air-Conditioned Rooms at Different Heat Loads. *Building Service Engineering Research & Technology, Vol. 1, No. 4.*

Nielsen, P.V. [1983]: Air Diffusion in Rooms with Ceiling-Mounted Obstacles and Two-Dimensional Isothermal Flow. *16th International Congress of Refrigeration, Commission E1, Paris.*

Nielsen, P.V. [1988]: Personal Communication. *Aalborg University.*

Nielsen, P.V. [1990]: Air Velocity at the Floor in a Room with Wall Mounted Air Terminal Device and Displacement Ventilation. *(in Danish). Internal Report, Nordic Ventilation Group, ISSN 0902-7513 R9004, Aalborg University, Aalborg.*

Nielsen, P.V. [1992]: Velocity Distribution in the Flow from a Wall-Mounted Diffuser in Rooms with Displacement Ventilation. *Proc. of the Third International Conference on Air Distribution in Rooms. ROOMVENT '92, Aalborg.*

Nielsen, P.V. [1994a]: Velocity Distribution in a Room with Displacement Ventilation and Low-Level Diffusers. *Internal IEA-Annex 20 Report, Aalborg University, ISSN 0902-7513 R9403.*

Nielsen, P.V. [1994b]: Stratified Flow in a Room with Displacement Ventilation and Wall Mounted Air Terminal Devices. *ASHRAE Transactions, Vol. 100, part 1, pp* .

Nielsen, P.V.; Hoff, L.; Pedersen, L.G. [1988]: Displacement Ventilation by Different Types of Diffusers. *9th AIVC Conference on Effective Ventilation, Gent, Belgium.*

Nielsen, P.V.; Möller, Å.T.A. [1985]: Measurements of the three-dimensional wall jet from different types of air diffusers. *Clima 2000, Copenhagen.*

Nielsen, P.V.; Möller, Å.T.A. [1987]: Measurements on Buoyant Wall Jet Flows in Air-conditioned Rooms. *ROOMVENT '87, International Conference on Air Distribution in Ventilated Spaces, Stockholm.*

Nielsen, P.V.; Möller, Å.T.A. [1988]: Measurements on Buoyant Jet Flows from a Ceiling Mounted Slot Diffuser. *Proc. of the 3rd Seminar on "Application of Fluid Mechanics in Environmental Protection - 88", Silesian Technical University.*

Popiolek, Z. [1996]: Air Volume Flux in Buoyant Plumes. *Silesian Technical University, Gliwice, Poland.*

Rajaratnam, N. [1976]: Turbulent Jets. *Elsevier, Amsterdam.*

Regenscheit, B. [1959]: Die Luftbewegung in Klimatisierten Räumen. *Kältetechnik, Heft 1.*

Regenscheit, B. [1970]: Die Archimedes-zahl. *Gesundheits Ingenieur, Heft 6.*

Sandberg, M.; Mattsson, M. [1993]: Density Currents created by Supply from Low Velocity Devices. *Research Report TN:44, The National Swedish Institute for Building Research..*

Schwenke, H. [1975]: Über das Verhalten ebener Horizontaler Zuluftstrahlen im begrenzten Raum. *Luft und Kältetechnik, 1975/5, pp 241-245.*

Schwenke, H. [1976]: Berechnung Lüftungstechnischer Anlagen. *ILKA Berechnungs-Katalog. Institut für Luft- und Kältetechnik, Dresden.*

Shillinglaw, J.A. [1977]: Cold Window Surfaces and Discomfort. *BSE, Vol. 45, pp 43-51.*

Skistad, H. [1993]: Private Communication.

Skistad, H. [1994]: Displacement Ventilation. *John Wiley & Sons Inc.*

Skåret, E. [1976]: Air Movement in Ventilated Rooms (in Norwegian). *Institute for VVS, Technical University of Norway, Trondheim.*

Skåret, E. [1986]: Ventilation by Displacement - Characterisation and Design Implications. *Ventilation '85, edited by H. D. Goodfellow, Elsevier Science Publishers B.V., Amsterdam.*

Söllner, G. and Klingenberg, K. [1972]: Leuchten als Störkörper im Luftstrom. *HLII, 23, no. 4, 1972.*

Topp, C.; Heiselberg, P. [1996]: Obstacles - an Energy-Efficient Method to Reduce Downdraught from Large Glazed Surfaces. *Proc. of the Fifth International Conference on Air Distribution in Rooms, ROOMVENT'96, Yokohama, Japan.*

Vialle, P.; Blay, D. [1996]: Decay Laws in the Case of 3D Vertical Free Jets with Positive Buoyancy. *ROOMVENT '96, Yokohama, July 17-19, Japan.*

Wilkinson, D.L.; Wood, I.R. [1970]: A rapidly varied Flow Phenomenon in a Two-Layer Flow. *J. Fluid Mech., Vol. 47, part 2, pp241-256.*

PAPERS ON INDOOR ENVIRONMENTAL TECHNOLOGY

PAPERS ON INDOOR ENVIRONMENTAL TECHNOLOGY

PAPER NO. 52: Lars Davidson & Peter V. Nielsen: *Calculation of the Two-Dimensional Airflow in Facial Regions and Nasal Cavity using an Unstructured Finite Volume Solver.* ISSN 1395-7953 R9539.

PAPER NO. 53: Henrik Brohus & Peter V. Nielsen: *Personal Exposure to Contaminant Sources in a Uniform Velocity Field.* ISSN 1395-7953 R9540.

PAPER NO. 54: Erik Bjørn & Peter V. Nielsen: *Merging Thermal Plumes in the Indoor Environment.* ISSN 1395-7953 R9541.

PAPER NO. 55: K. Svidt, P. Heiselberg & O. J. Hendriksen: *Natural Ventilation in Atria - A Case Study.* ISSN 1395-7953 R9647.

PAPER NO. 56: K. Svidt & B. Bjerg: *Computer Prediction of Air Quality in Livestock Buildings.* ISSN 1395-7953 R9648.

PAPER NO. 57: J. R. Nielsen, P. V. Nielsen & K. Svidt: *Obstacles in the Occupied Zone of a Room with Mixing Ventilation.* ISSN 1395-7953 R9649.

PAPER NO. 58: C. Topp & P. Heiselberg: *Obstacles, an Energy-Efficient Method to Reduce Downdraught from Large Glazed Surfaces.* ISSN 1395-7953 R9650.

PAPER NO. 59: L. Davidson & P. V. Nielsen: *Large Eddy Simulations of the Flow in a Three-Dimensional Ventilated Room.* ISSN 1395-7953 R9651.

PAPER NO. 60: H. Brohus & P. V. Nielsen: *CFD Models of Persons Evaluated by Full-Scale Wind Channel Experiments.* ISSN 1395-7953 R9652.

PAPER NO. 61: H. Brohus, H. N. Knudsen, P. V. Nielsen, G. Clausen & P. O. Fanger: *Perceived Air Quality in a Displacement Ventilated Room.* ISSN 1395-7953 R9653.

PAPER NO. 62: P. Heiselberg, H. Overby & E. Bjørn: *Energy-Efficient Measures to Avoid Downdraft from Large Glazed Facades.* ISSN 1395-7953 R9654.

PAPER NO. 63: O. J. Hendriksen, C. E. Madsen, P. Heiselberg & K. Svidt: *Indoor Climate of Large Glazed Spaces.* ISSN 1395-7953 R9655.

PAPER NO. 64: P. Heiselberg: *Analysis and Prediction Techniques.* ISSN 1395-7953 R9656.

PAPER NO. 65: P. Heiselberg & P. V. Nielsen: *Flow Element Models.* ISSN 1395-7953 R9657.

PAPER NO. 66: Erik Bjørn & P. V. Nielsen: *Exposure due to Interacting Air Flows between Two Persons.* ISSN 1395-7953 R9658.

PAPER NO. 67: P. V. Nielsen: *Temperature Distribution in a Displacement Ventilated Room.* ISSN 1395-7953 R9659.

PAPER NO. 68: G. Zhang, J. C. Bennetsen, B. Bjerg & K. Svidt: *Analysis of Air Movement Measured in a Ventilated Enclosure.* ISSN 139995-7953 R9660.